Comparison of $CeBr_3$ with $LaBr_3$:Ce, $LaCl_3$:Ce, and NaI:Tl Detectors

Paul Guss[a], Michael Reed[a], Ding Yuan[a],
Matthew Cutler[b], Chris Contreras[b], and Denis Beller[b]
[a]Remote Sensing Laboratory, P.O. Box 98521, M/S RSL-13, Las Vegas, NV 89193,
gusspp@nv.doe.gov
[b]University of Nevada, Las Vegas, 4505 S. Maryland Parkway, Las Vegas, NV 89154,
bellerd@unlv.nevada.edu

ABSTRACT

Energy resolution and detection efficiency were compared between two sizes of cerium bromide ($CeBr_3$) scintillators, three sizes of lanthanum bromide ($LaBr_3$:Ce) scintillators, three sizes of sodium iodide (NaI:Tl) scintillators, and a lanthanum chloride ($LaCl_3$:Ce) scintillator. Comparisons are made of key parameters such as energy resolution, detection efficiency, linearity, and self-activity of $CeBr_3$, $LaBr_3$:Ce, $LaCl_3$:Ce, and NaI:Tl scintillator detectors. The scintillator detectors are tested by comparing the peak separation and identification in the energy range up to 3.0 MeV using ^{133}Ba, ^{152}Eu, and naturally occurring radioactive materials [1]. The study has shown that $CeBr_3$ scintillator detectors provided by Saint-Gobain offer better resolution than NaI:Tl scintillator detectors. $CeBr_3$ detectors could resolve some closely spaced peaks from ^{133}Ba and ^{152}Eu, which NaI:Tl could not. $LaBr_3$:Ce has slightly better resolution, and a slightly higher efficiency than $CeBr_3$. In this work, "self-activity" of each of these four detector types was measured by operating the detectors themselves. A comparison of the intrinsic activity for all of the detectors in this study is demonstrated. For $CeBr_3$, the self-activity present may be reduced, or even eliminated in the future, through improved processes for growing the material. It will be discussed if, and under what conditions, $CeBr_3$ may be better than $LaBr_3$:Ce and $LaCl_3$:Ce for detection of certain special nuclear material γ-rays [2]. An overall advantage of $CeBr_3$ detectors over lanthanum halide and NaI:Tl detectors will be discussed.

Keywords: $CeBr_3$, $LaBr_3$:Ce, $LaCl_3$:Ce, NaI:Tl, efficiency, gamma spectral comparison, resolution.

1. INTRODUCTION

Comparisons of room-temperature cerium doped lanthanum bromide ($LaBr_3$:Ce), cerium doped lanthanum chloride ($LaCl_3$:Ce), and thallium doped sodium iodide (NaI:Tl) scintillator detectors have been made to cadminum zinc telluride (CZT) and high-purity germanium (HPGe) detectors [1]. In this work, these comparisons have been extended to include a relatively newer scintillator detector, cerium bromide ($CeBr_3$), based on interesting results obtained in recent studies [2]. New scintillators, activated with cerium (Ce) ions as the primary scintillation source such as $LaBr_3$:Ce and $LaCl_3$:Ce have gained interest due to good time resolution (100 to 600 picoseconds depending on crystal size), good energy resolution (2%–3% full width at half maximum [FWHM] at 661 keV), high efficiency and light output per keV (63 photons/keV), and fast decay time (16 ns) [1], [3]. These superior properties classify these materials as possible radiation detectors that could replace CZT and NaI:Tl for a variety of applications requiring detectors that operate at room temperature. The shortcoming of $LaBr_3$:Ce and $LaCl_3$:Ce scintillators is that they are slightly "self-active," which can be seen as spurious spectral lines when collecting a spectrum. These intrinsic spurious lines may limit the utilization of the detector, especially in low-level counting. The "self-activity" is due to the presence of the unstable ^{138}La isotope, uranium, and actinium series contaminant [2], [4]–[5]. It has been mentioned that the uranium and actinium series contaminant in the most recent $LaBr_3$:Ce scintillators has been reduced greatly [4], [6]. In this work, "self-activity" of $LaBr_3$:Ce was measured by operating the detector itself. As it turns out, $CeBr_3$ shares many of the positive properties of $LaBr_3$:Ce and $LaCl_3$:Ce of good time resolution, good energy resolution, high efficiency and light output per keV, and fast decay time, but with a reduced self-activity [2]. Comparisons are made of key parameters such as energy resolution and detection efficiency of $CeBr_3$, $LaBr_3$:Ce, $LaCl_3$:Ce, and NaI:Tl detectors. The scintillator detectors are tested by comparing the peak separation and identification in the energy range up to 1.5 MeV using ^{133}Ba, ^{152}Eu, and naturally occurring radioactive materials (NORM). The motivation of this study is to evaluate $CeBr_3$, $LaBr_3$:Ce, $LaCl_3$:Ce, and

Hard X-Ray, Gamma-Ray, and Neutron Detector Physics XII, edited by Arnold Burger, Larry A. Franks, Ralph B. James,
Proc. of SPIE Vol. 7805, 78050L · © 2010 SPIE · CCC code: 0277-786X/10/$18 · doi: 10.1117/12.862579

2. EXPERIMENT

2.1 Scintillator Detectors

Part of this work included growing large crystals of the scintillator $CeBr_3$ and evaluating their properties. Three $CeBr_3$ crystals were grown and coupled to photomultiplier tubes; the first crystal measured ½″ × ½″, and the other two crystals were each 1″ × 1″. Radiation Monitoring Devices, Inc. (RMD) has fabricated and used a ½″ × ½″ $CeBr_3$ crystal [10-11]. They provided their crystal to Saint-Gobain for this work in order to assist Saint-Gobain in growth and benchmarking of a new crystal for this study [12]. Fig. 1 is a picture of the ½″ × ½″ crystal grown at Saint-Gobain. All of these crystals were used for comparisons with $LaBr_3$:Ce and NaI:Tl in each of three different size crystal dimensions. Another material, $LaCl_3$:Ce, which included impurities of rare earth metals, was also compared for performance and self-activity [13]. In total, 10 different crystals are depicted in Table 1 for these experiments: $CeBr_3$ (½″ × ½″), $CeBr_3$ (1″ × 1″), $LaBr_3$:Ce (1″ × 1″), $LaBr_3$:Ce (2″ × 2″), $LaBr_3$:Ce (3″ × 3″), $LaCl_3$:Ce (1″ × 1″), NaI:Tl (1″ × 1″), NaI:Tl (2″ × 2″), and NaI:Tl (3″ × 3″).

Figure 1. The ½″ × ½″ $CeBr_3$ crystal epoxied to a photomultiplier tube [2].

Table 1. Summary of the different crystal sizes used in this study.

Crystal	½″ × ½″	1″ × 1″	2″ × 2″	3″ × 3″	Total
$CeBr_3$ 1 2	3	--			
$LaBr_3$:Ce	3	1			
$LaCl_3$:Ce	--	1	1	--	
NaI:Tl	3 1 --	1 1			
Total	21	3	10		
Volume per Crystal (cc)	0.1	0.78	6.2	21.2	

2.2 Data Acquisiton

The scintillation detectors were coupled with a photomultiplier tube (for the 1″ × 1″ cerium and lanthanum halide detectors a Photonis XP2060B photomultiplier tube was used) and a preamplifier was obtained from Saint-Gobain. The assembly was connected to and powered by the ORTEC DigiDART. Operation bias of the scintillators and the conversion gain were set to establish 1 keV per channel. A "self activity" spectrum was also taken of each of the scintillators, including NaI:Tl, for periods extending over one day in a low-background lead pyramid to illustrate the internal (self) detection of the intrinsic decay spectrum of La and possibly alpha particles from the uranium decay chain.

In this work, each of two sizes of $CeBr_3$ crystals were obtained and benchmarked against NaI:Tl and $LaBr_3$:Ce. This work also benchmarked a $LaCl_3$:Ce crystal. The team documented energy resolution and counting efficiency characteristics using a series of isotopes and γ-ray energies (^{22}Na, ^{60}Co, ^{137}Cs, ^{133}Ba, ^{152}Eu, ^{207}Bi, ^{228}Th, ^{241}Am, depleted uranium [DU], highly enriched uranium [HEU], and weapons-grade plutonium [Pu]). These isotopes gave a reasonable

coverage of energy range for overall performance evaluation. All sources used were "point sources." For each source spectrum, all radioisotopic sources were placed 40 cm from the detector inside a shielding safe with 1″ of lead on all six faces of the safe. Both detector and source were located inside the lead safe. Source strength in the 1–100 μ Ci range was chosen in each case to highlight the difficulty of seeing the signal from a weak source in the presence of a high internal background. This simulates a situation as when a large amount of detector material (and hence large amounts of self-activity) is involved for detector configurations used for high sensitivity or long-range interrogation missions.

3. RESULTS AND DISCUSSION

3.1 Intrinsic Spectral Analysis

Preliminary estimates of self-activity, resolution, intrinsic efficiency, size effect, and linearity were defined [2].

Fig. 2 displays the background spectra obtained with the 1″ × 1″ $CeBr_3$ detector taken inside the University of Nevada, Las Vegas (UNLV) Lead Shielding Pyramid, shown in Fig. 3, which was constructed for this project. It provided no less than 2″ of lead on all sides of the detector. This count was taken for 115 hours in the low background UNLV Lead Shielding Pyramid (Fig. 3), and the spectrum in Fig. 2 represents the gross sum of counts for this period. Notice that the ^{40}K peak at 1461 keV stands out. Notice also the peaks at 1675 keV and 1903 keV. These peaks appeared in the spectrum for the ½″ × ½″ $CeBr_3$ detector as well. These two energy peaks do not appear to have an associated Compton edge, leading to speculation of some sort of correlation with α activity associated with the detector. There is not a clear or readily self-evident explanation for these peaks, making them an interesting area of study of the associated physics on its own merit.

Figs. 2 and 4 are spectra acquired for a 1″ × 1″ $CeBr_3$ crystal and a 1″ × 1″ $LaBr_3$:Ce crystal, respectively, for comparison. Fig. 4 shows the background spectrum measured with the $LaBr_3$:Ce detector after over 67 hours in the low background UNLV Lead Shielding Pyramid. Three intrinsically produced photon peaks from the decay of ^{138}La were observed. These are the 789 keV γ line from the β decay branch, the 1436 keV γ line from the electron capture branch, and a 32 keV X-ray fluorescence peak. A 1461 keV line from ^{40}K, with a much smaller scale, is present (i.e., see the measurement made in Fig. 2 without the ^{138}La background lines) but difficult to observe next to the 1436 keV line. One immediately sees the features associated with the intrinsic activity for $LaBr_3$:Ce from the background count. These features include the 789 keV γ -ray peak, along with an associated β decay spectrum (0–255 keV), and the 1436 keV γ-ray peaks, along with an associated a 32 keV X-ray. In fact, the 32 keV X-ray may be emitted nearly in coincidence with 1436 keV γ-ray, creating a comingled signature at the sum energy of 1468 keV in proximity to the 1436 keV line and the ^{40}K line at 1461 keV, leading to the rather large width of this "peak." The same phenomena of near coincidence signatures occurs between the 789 keV γ-ray and the β decay spectrum (0–255 keV), leading to the feature between 789 keV and 1 MeV, which is hardy Gaussian in shape yet is predominately correlated to a monoenergetic 789 keV γ-ray.

The "self activity" and background spectrum of the $LaBr_3$:Ce scintillator is shown in Fig. 4. The continuum with an endpoint at approximately 255 keV is probably due to the β decay of ^{138}La to ^{138}Ce. The emission line with a peak around 1461 keV corresponds to the overlapped 1461 keV line of ^{40}K, originating from the glass of the photomultiplier tube, with the 1436 keV ^{138}La line summing internally with 32 keV X-rays. The 789 keV line sitting on the β continuum is only just resolvable. The low-energy photon peak at approximately 32 keV is due to ^{138}Ba $K_{\alpha 1}$ (32.2 keV) and $K_{\alpha 2}$ (31.8 keV) X-ray fluorescence. ^{138}Ba is the daughter product of ^{138}La from the electron capture branch. The broad band peaks (between 1700 and 2700 keV) due to alpha particles from the uranium decay chain [2], [4]–[5] are also observed (Fig. 2).

In Fig. 5, results for the self-activity are shown as a function of the size of the $LaBr_3$:Ce crystal. Fig. 6 is a compelling spectral comparison that argues for $CeBr_3$. Our work documented a lower background with $CeBr_3$ than with either $LaBr_3$:Ce or $LaCl_3$:Ce, for the energy region of interest when looking for γ-rays associated with manmade radioisotopes. The intrinsic background observed in the $CeBr_3$ spectra is mostly due to contaminants associated with α signatures that are evident in Fig. 2. In the critical low-energy areas of the spectrum, where the lower energy special nuclear material (SNM) peaks occur, the $CeBr_3$ had a reduction in intrinsic background.

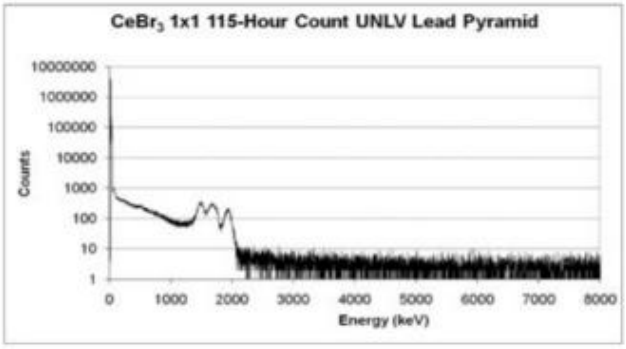

Figure 2. Background gamma-ray spectrum using the 1″ × 1″ $CeBr_3$ detector taken inside the UNLV Lead Shielding Pyramid. This count was taken for 115 hours.

Figure 3. Background and self-activity gamma-ray spectra are acquired at UNLV using this "UNLV Lead Shielding Pyramid.

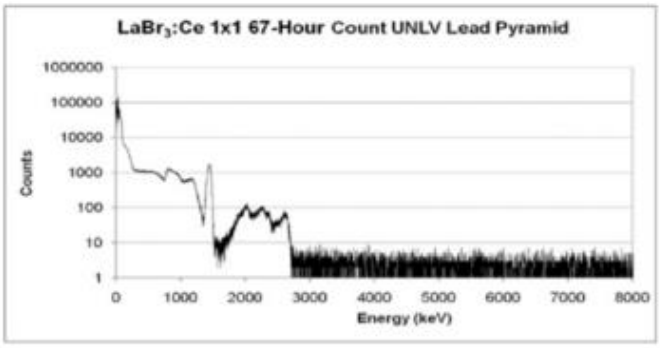

Figure 4. Background gamma-ray spectrum using the 1″ × 1″ $LaBr_3$:Ce detector taken inside the UNLV Lead Shielding Pyramid. This count was taken for 67 hours Pyramid."

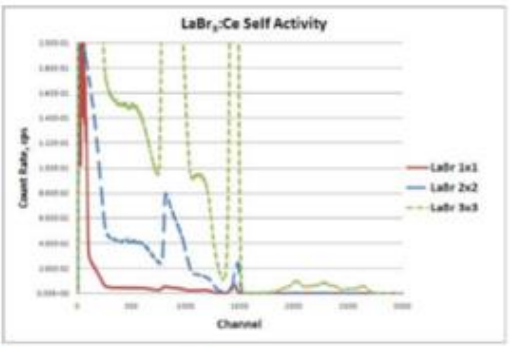

Figure 5. Background and self-activity gamma-ray spectra acquired for 3 sizes of $LaBr_3$:Ce detectors using the " UNLV Lead Shielding

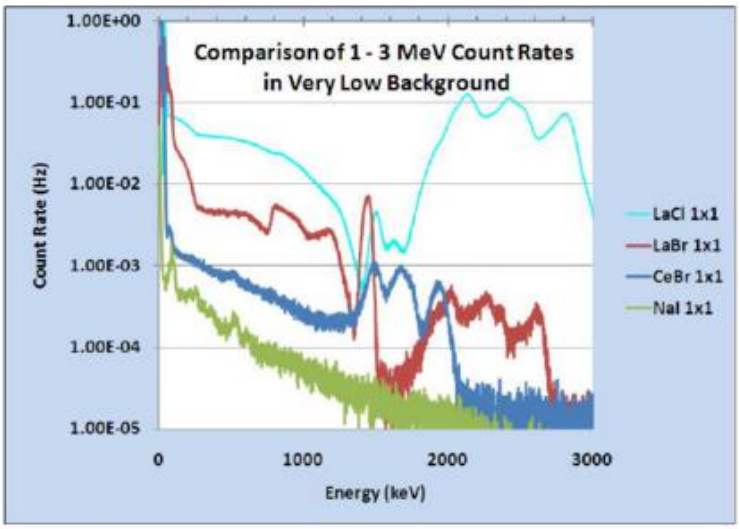

Figure 6. Comparison of the intrinsic "self-activity" for each of the $CeBr_3$, $LaBr_3$:Ce, $LaCl_3$:Ce, and NaI:Tl scintillator detectors [2].

3.2 Energy Resolution Comparison

The energy resolutions of $CeBr_3$, $LaBr_3$:Ce, $LaCl_3$:Ce were compared with the resolution of NaI:Tl. Before discussing energy resolution, we would like to note that generally smaller scintillation crystals produce a better resolution. Also good spectral resolution is required for isotopic identification, particularly when peaks are closely grouped together as in HEU and Pu, or for identification of isotopes in mixed sources.

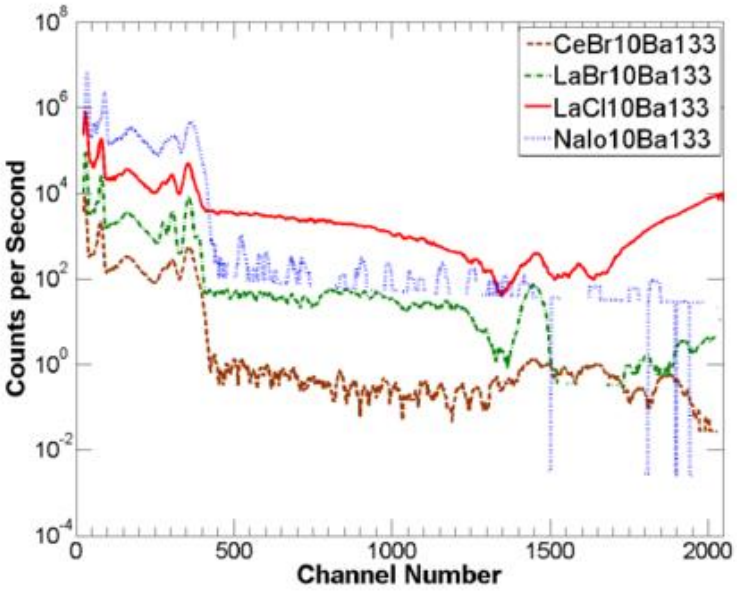

Figure 7. ^{133}Ba (6 μCi) energy spectrum comparison between 1″ × 1″ $CeBr_3$, $LaBr_3$:Ce, $LaCl_3$:Ce, and NaI:Tl detectors [2]. Each detector is plotted on a successive decade to allow comparison. To obtain actual number of counts measured per second, divide $CeBr_3$ spectrum by 10^3, $LaBr_3$:Ce spectrum by 10^4, $LaCl_3$:Ce spectrum by 10^5, and NaI:Tl spectrum by 10^6.

For example, ^{133}Ba has four main peaks grouped closely together (separated by less than 100 keV) showing the importance of adequate spectral resolution for isotopic identification. In Fig. 7, the NaI:Tl detector is unable to resolve all four key peaks of ^{133}Ba, namely 276, 303, 356, and 383 keV. The $LaBr_3$:Ce and $LaCl_3$:Ce detectors are able to resolve these emission line groupings. The four peaks could be extracted from the $CeBr_3$ if good peak fitting routines are used. Interestingly in Fig. 7, it can be observed that when the source is sufficiently small enough (6 μCi of ^{133}Ba), then the curves of the NaI:Tl and $LaBr_3$:Ce cross, even though the NaI:Tl is plotted against a higher decade. This is indicative of the high values of "self-activity" of the lanthanum halide detectors and of how this self-activity may reduce sensitivity to very small sources.

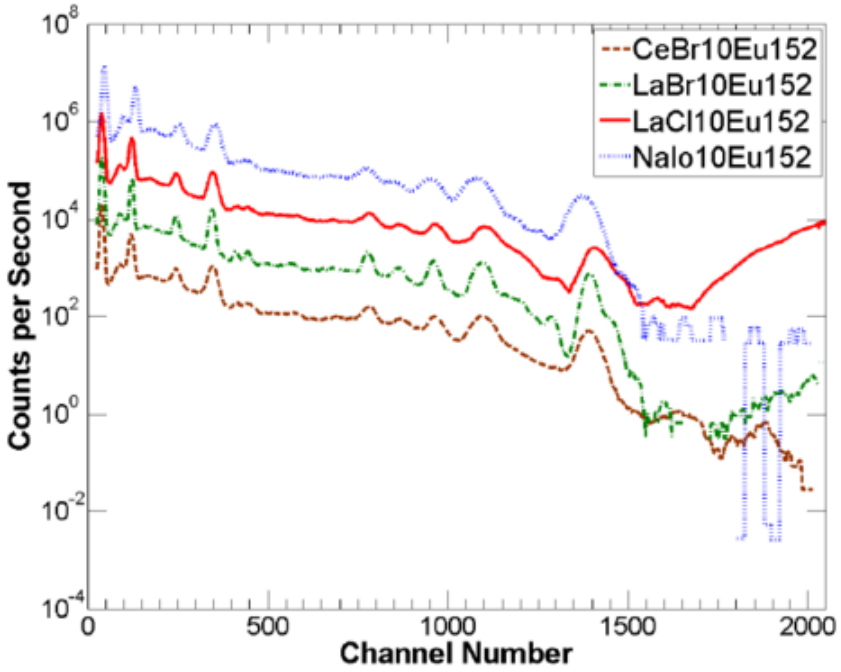

Figure 8. ^{152}Eu (24 μCi) energy spectrum comparison between 1″ × 1″ $CeBr_3$, $LaBr_3$:Ce, $LaBr_3$:Ce, and NaI:Tl detectors [2]. Each detector is plotted on a successive decade to allow comparison. To obtain actual number of counts measured per second, divide $CeBr_3$ spectrum by 10^3, $LaBr_3$:Ce spectrum by 10^4, $LaCl_3$:Ce spectrum by 10^5, and NaI:Tl spectrum by 10^6.

Good spectral resolution and high efficiency becomes important when working with sources that have a complicated decay scheme. For example, ^{152}Eu has a complicated decay scheme that has emissions over a large range of energy, with relatively close peaks at both ends of this energy range. As seen in Fig. 8, $CeBr_3$, $LaBr_3$:Ce, and $LaCl_3$:Ce were able to resolve closely spaced emission lines of Eu, such as 411 and 444 keV lines. When a similar ^{152}Eu spectrum was taken with NaI:Tl, these close spectral lines could not be resolved. Notice also that the 1436 keV related cluster associated with the lanthanum halide detectors interferes with production of a clean Gaussian peak for the 1408 keV γ-ray line in ^{152}Eu spectra, whereas this peak is more clearly defined without interference using the $CeBr_3$ or the NaI:Tl detectors. In Figs. 9 and 10, comparisons are made for DU and HEU, respectively. Fig. 11 shows the greater ability of the $CeBr_3$, $LaBr_3$:Ce, and $LaCl_3$:Ce detectors over the NaI:Tl detector in resolving the ^{239}Pu γ-ray photopeaks in the region of 300 to 414 keV. For the ^{239}Pu isotope, the peaks were on a larger background when acquired with the $LaBr_3$:Ce or a $LaCl_3$:Ce crystal. The signal-to-noise ratio was better for the 1" × 1" $CeBr_3$ detector than for these other two detectors. Fig. 12 illustrates the variations of energy resolution (defined as FWHM/E) of the detectors as a function of the γ energies. The best fit of the $CeBr_3$, $LaBr_3$:Ce, and $LaCl_3$:Ce data is shown in Fig. 12, providing another comparison between the $CeBr_3$, $LaBr_3$:Ce, $LaCl_3$:Ce, and NaI:Tl detectors. Our fit is not an ideal inversely proportional function of the square root of the energy [5, 9].

In general, $CeBr_3$ is a good compromise between the $LaBr_3$:Ce, $LaCl_3$:Ce, and NaI:Tl detectors with $CeBr_3$, $LaBr_3$:Ce, and $LaCl_3$:Ce slightly outperforming NaI:Tl. As seen in Fig. 12, the resolution of the $CeBr_3$, $LaBr_3$:Ce, and $LaCl_3$:Ce detectors appears to be excellent for energies above approximately120 keV; whereas below 120 keV, the resolution becomes similar to NaI:Tl, as described in the publication [5]. For energies below 120 keV, $CeBr_3$, $LaBr_3$:Ce, and $LaCl_3$:Ce offer little advantage over NaI:Tl. Moreover, when considering the cost of the scintillator, NaI:Tl could be preferable over $CeBr_3$, $LaBr_3$:Ce, and $LaCl_3$:Ce. The resolution of the ^{137}Cs 662 keV line for NaI:Tl is 7% compared with 3.4% for $LaBr_3$:Ce, 4.4% for $LaCl_3$:Ce, and 5.8% for $CeBr_3$ (Fig. 12). This demonstrates that $CeBr_3$, $LaBr_3$:Ce, and $LaCl_3$:Ce detectors have clear advantages over the properties of the NaI:TI detector. Others have reported measuring the ^{137}Cs 662 keV line with a 4.9% resolution using $CeBr_3$ [14]. With regard to naturally occurring radioactive materials, a leading concern with the lanthanum halides is the interference between the cluster of 1436 keV to 1468 keV signatures due to ^{138}La and ^{40}K.

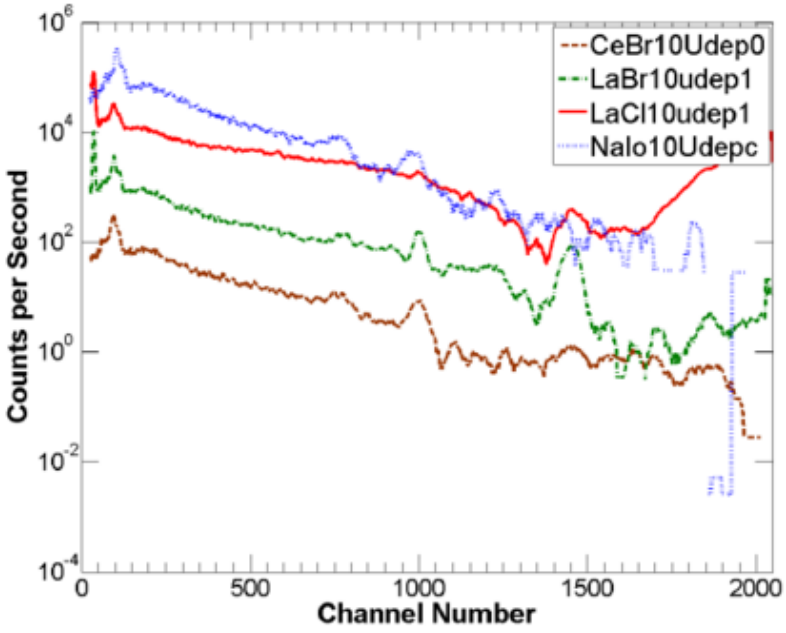

Figure 9. DU (154 μCi) energy spectrum comparison between 1″ × 1″ $CeBr_3$, $LaBr_3$:Ce, $LaCl_3$:Ce, and NaI:Tl detectors [2]. Each detector is plotted on a successive decade to allow comparison. To obtain actual number of counts measured per second, divide $CeBr_3$ spectrum by 10^3, $LaBr_3$:Ce spectrum by 10^4, $LaCl_3$:Ce spectrum by 10^5, and NaI:Tl spectrum by 10^6.

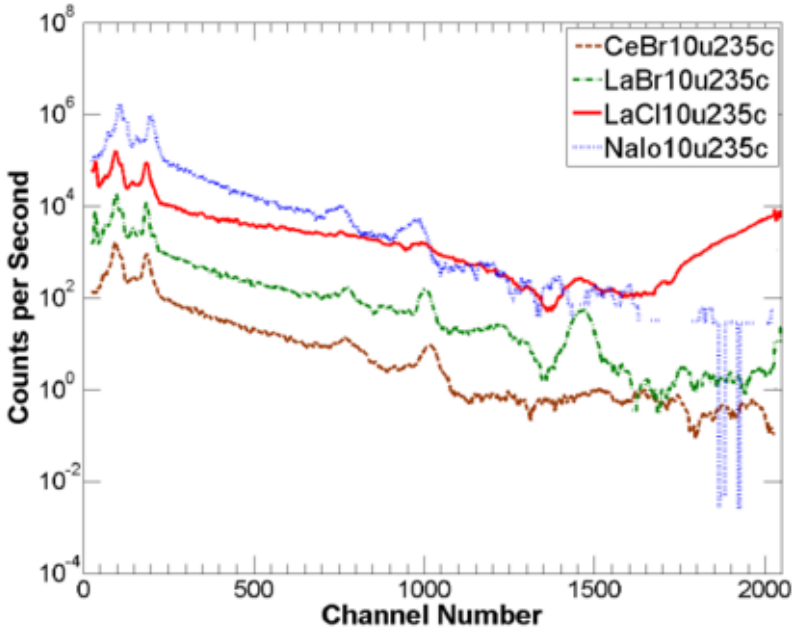

Figure 10. ^{235}U (100 μCi) energy spectrum comparison between 1″ × 1″ $CeBr_3$, $LaBr_3$:Ce, $LaCl_3$:Ce, and NaI:Tl detectors [2]. Each detector is plotted on a successive decade to allow comparison. To obtain actual number of counts measured per second, divide $CeBr_3$ spectrum by 10^3, $LaBr_3$:Ce spectrum by 10^4, $LaCl_3$:Ce spectrum by 10^5, and NaI:Tl spectrum by 10^6.

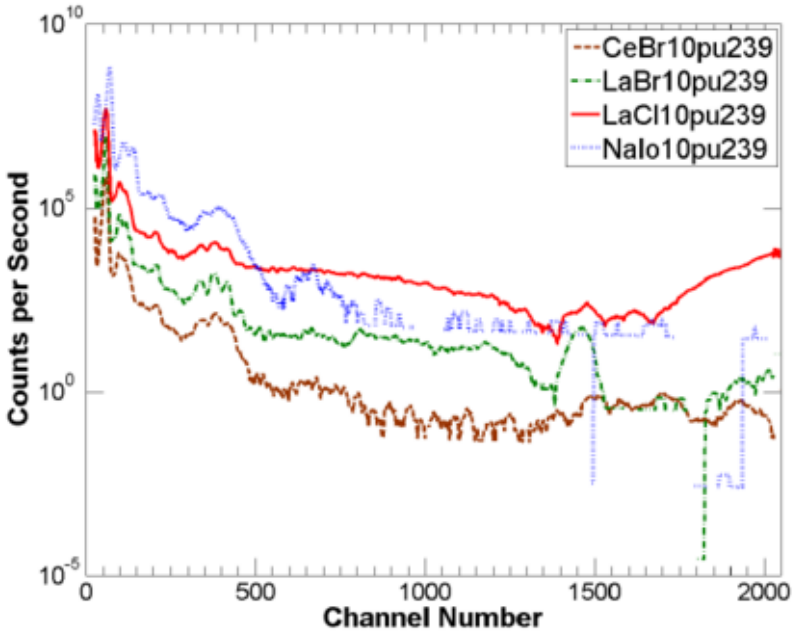

Figure 11. ^{239}Pu (2 μCi) energy spectrum comparison between 1″ × 1″ $CeBr_3$, $LaBr_3$:Ce, $LaCl_3$:Ce, and NaI:Tl detectors [2]. Each detector is plotted on a successive decade to allow comparison. To obtain actual number of counts measured per second, divide $CeBr_3$ spectrum by 10^3, $LaBr_3$:Ce spectrum by 10^4, $LaCl_3$:Ce spectrum by 10^5, and NaI:Tl spectrum by 10^6.

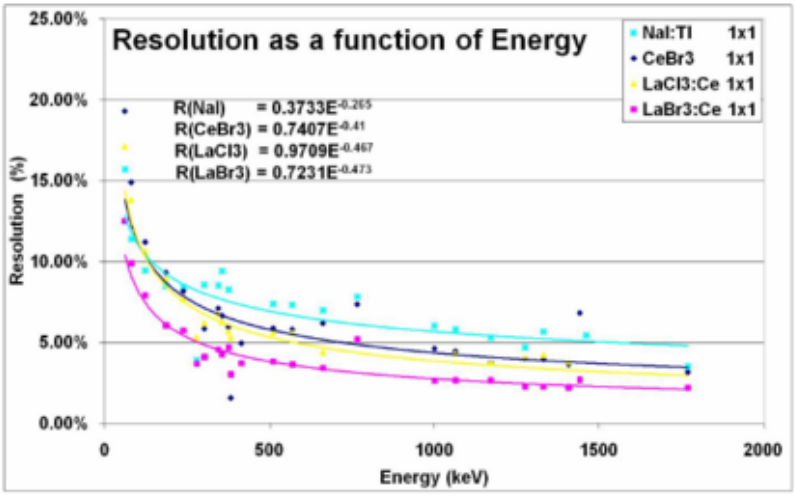

Figure 12. Energy resolution comparison between 1″ × 1″ $CeBr_3$, $LaBr_3$:Ce, $LaCl_3$:Ce, and NaI:Tl detectors [2].

3.3 Detection Efficiency Comparison

A comparison of the full energy peak relative intrinsic efficiency is shown in Fig. 13 for the four 1″ × 1″ $CeBr_3$, $LaBr_3$:Ce, $LaCl_3$:Ce, and NaI:Tl scintillator detectors in the energy range of 122 to 1408 keV. Figs. 14 and 15 plot the intrinsic efficiencies. Note that the larger detectors have a greater efficiency because their volume is larger. When comparing $LaBr_3$:Ce with $LaCl_3$:Ce, $LaBr_3$:Ce has a greater efficiency. When examining the data for $CeBr_3$, note that its efficiency is comparable to $LaBr_3$:Ce and better than the other two scintillators. In the high-energy regime (above approximately 1 MeV), the efficiency of the scintillators are similar.

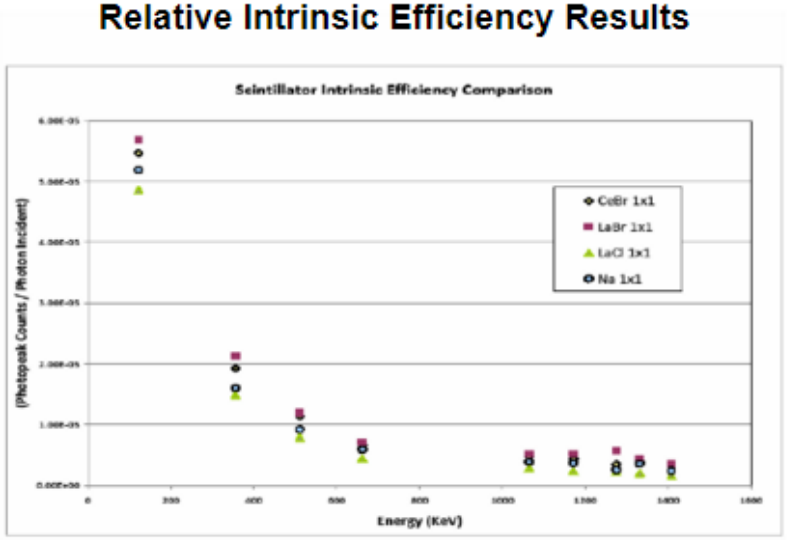

Figure 13. Relative intrinsic efficiency for $CeBr_3$ is comparable to other detector materials in class.

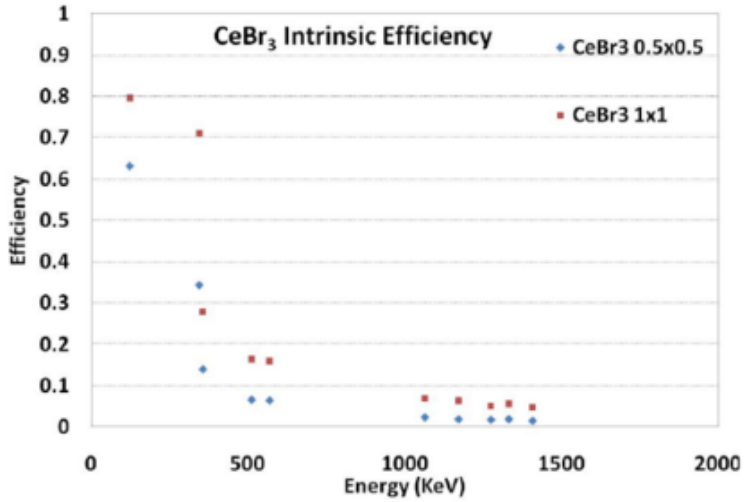

Figure 14. Intrinsic efficiency for $CeBr_3$ does increase with size of the crystal.

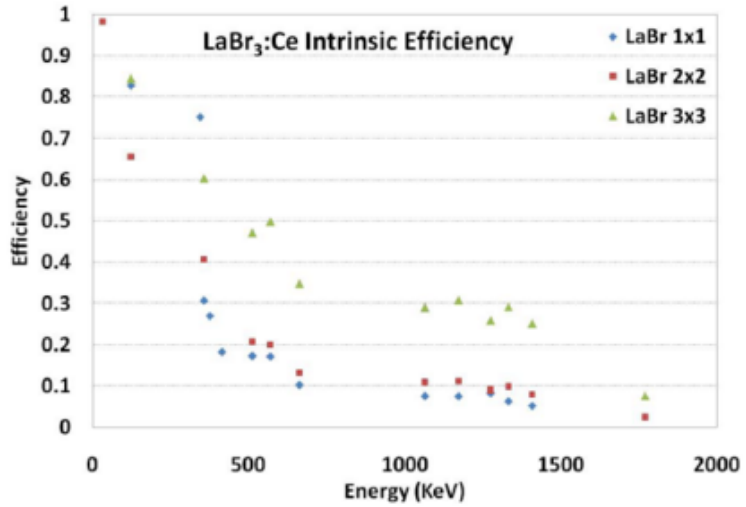

Figure 15. Intrinsic efficiency for $LaBr_3$:Ce also increases with size of the crystal.

3.4 Linearity

We measured the non-linearity of photon yield versus energy for the $CeBr_3$ detectors and determined the linearity (Fig.16) to be better than 2% in the 100–1500 keV energy range. The NaI:Tl non-linearity is an order of magnitude worse than for $CeBr_3$. This work also showed that the non-linearity for $LaBr_3$:Ce was somewhere in between these two extremes. This finding for $LaBr_3$:Ce is consistent with what has been reported [15]. We prepared a few additional plots as a linearity analysis in Figs. 17–23 for the ½″ × ½″ $CeBr_3$, the 1″ × 1″ NaI:Tl, and the 3″ × 3″ $LaBr_3$:Ce detectors and will give a brief interpretation of them.

Fig. 16, shows a plot of photon energy E_γ vs. Centroid channel number $Ch_{centroid}$ for the ½″ × ½″ $CeBr_3$ and 1″ × 1″ NaI:Tl detectors. Here the $Ch_{centroid}$ number is the channel number for which the centroid of the peak corresponding to E_γ

appears. We were investigating linearity (light yield) here. The problem with the plots that we made is that one cannot tell much by looking at them. To this end, we plotted the following:

$$\mathcal{F} \text{ vs. } E_\gamma$$

Where, E_γ is the known photon energy (γ or x-ray) arising from the measured source, and the value of the parameter $\mathcal{F}$ is defined as:

$$\mathcal{F} = (E_\gamma - Ch_{centroid}) / E_\gamma$$

This is a normalized residual of sorts. It is more meaningful if one looks at the plot (Fig. 17) of this figure of merit. Notice that the signs change and recall that, with a calibration of 1 keV per channel, the photopeak energy for the 662 keV ^{137}Cs γ has been placed in Channel 662. This means that the quasi-residual is 0 for ^{137}Cs. In instances where the value of $\mathcal{F}$ is negative, the peak centroid appeared to the right of where it would be with a linear detector. This means that there was proportionally more light than what would have been expected based on the ^{137}Cs light yield. In instances where the value of $\mathcal{F}$ is positive, the peak centroid appeared to the left of where it would be with a perfectly linear detector. This of course means that there was proportionally less light than what would have been expected based on the ^{137}Cs light yield. This method is a much better way of exhibiting linearity. It is normalized because, while being 5 channels off at ^{241}Am (60 keV) is unacceptable, at the same time 5 channels off at ^{228}Th (2.614 MeV) implies a smaller relative error in energy. Something to note about this is that for the plots in which there occurs many sign changes in the value of $\mathcal{F}$, one can conclude that the emission spectra itself is erratic. For instances in which the plot is very smooth (the NaI:Tl plot shown in Fig. 19), one can conclude that the light yield curve, although not extremely linear, is quite smooth. Specifically in regard to detector comparisons, Fig. 18 shows an absolute variance from linearity of up to ±5 channels for $CeBr_3$ over the 0–2 MeV energy range. However, a variance of over 40 channels is evident in Fig. 20 for the case of NaI:Tl over the same energy range, with Fig. 22 showing that $LaBr_3$:Ce is somewhere in between these extremes. The scatter in the non-linearity residues is much larger for NaI:Tl than for $CeBr_3$. These data indicate that the $CeBr_3$ detector is the most linear of those studied in this work over the 0–2 MeV energy range (using the experimental setup conditions described above, which results in a 1 keV/channel calibration).

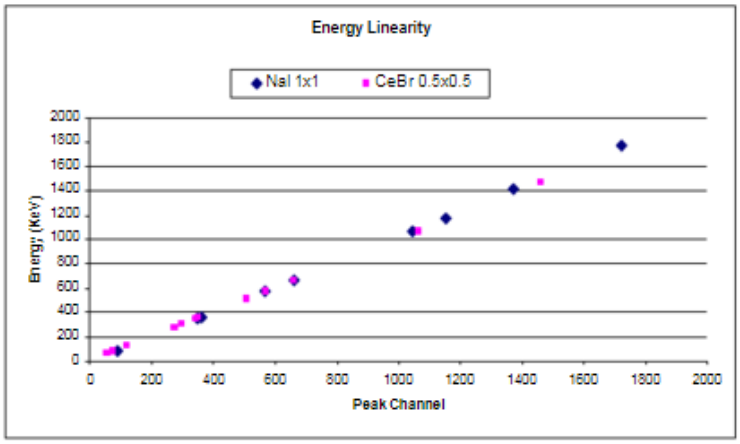

Figure 16. Linearity Plots of the NaI:Tl 1″ × 1″ and $CeBr_3$ ½″ × ½″ detector. Here the peak channel is plotted vs. the energy of the photon.

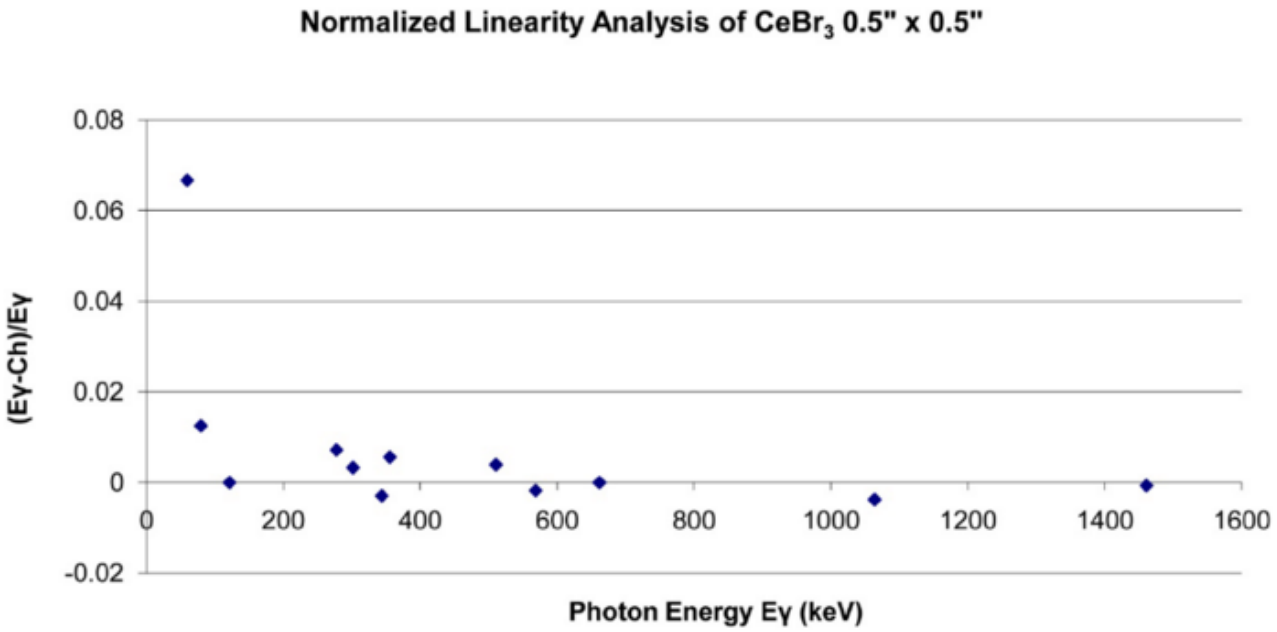

Figure 17. Normalized Linearity Analysis of the ½″ × ½″ $CeBr_3$ detector. Here the difference of the photon energy and channel divided by the photon energy is plotted against the photon energy.

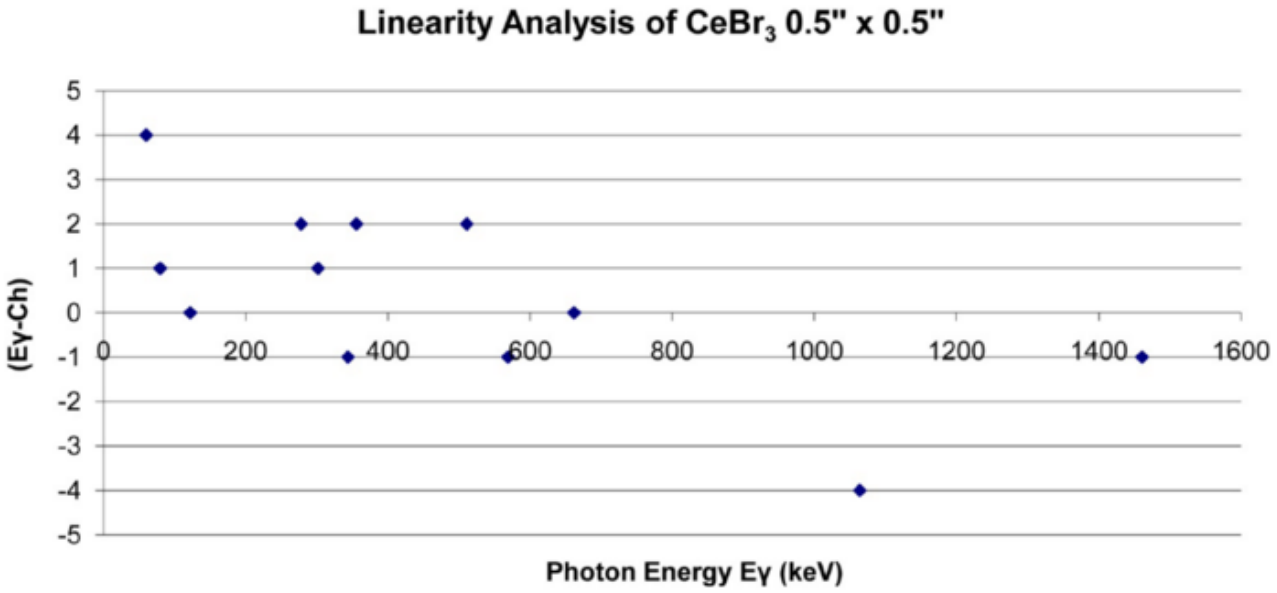

Figure 18. Linearity Analysis of the ½″ × ½″ $CeBr_3$ detector. Here the difference of the photon energy and channel is plotted against the photon energy.

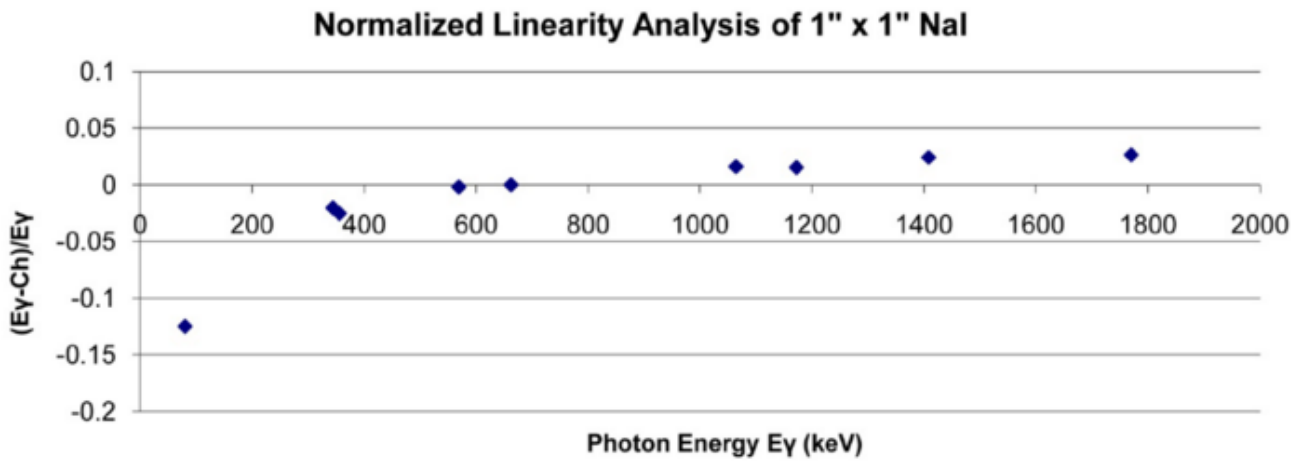

Figure 19. Normalized Linearity Analysis of the 1″ × 1″ NaI detector. Here the difference of the photon energy and channel divided by the photon energy is plotted against the photon energy.

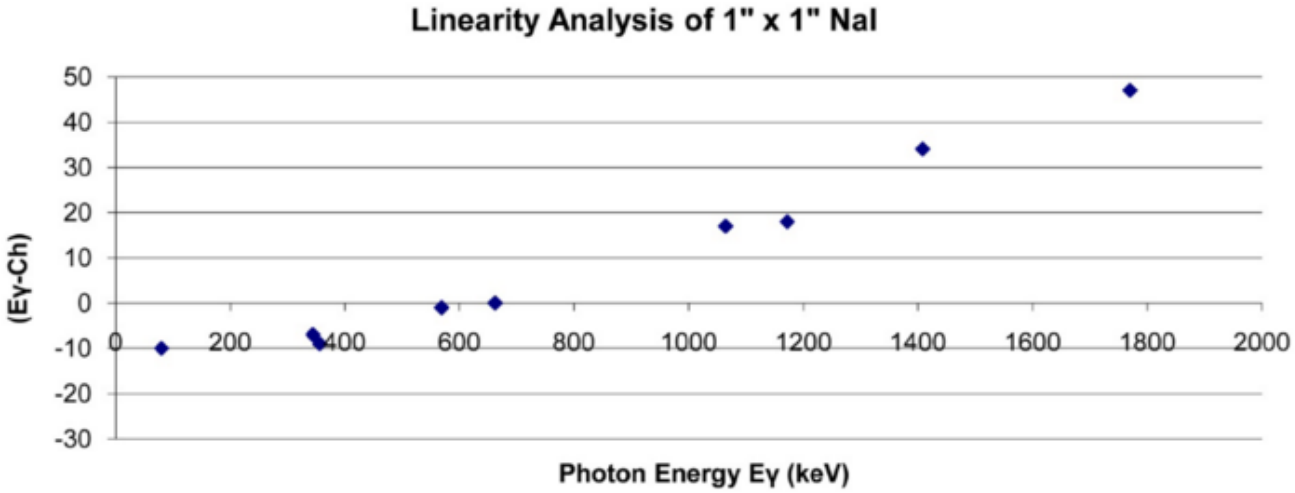

Figure 20. Linearity Analysis of the 1″ × 1″ NaI:Tl detector. Here the difference of the photon energy and channel is plotted against the photon energy.

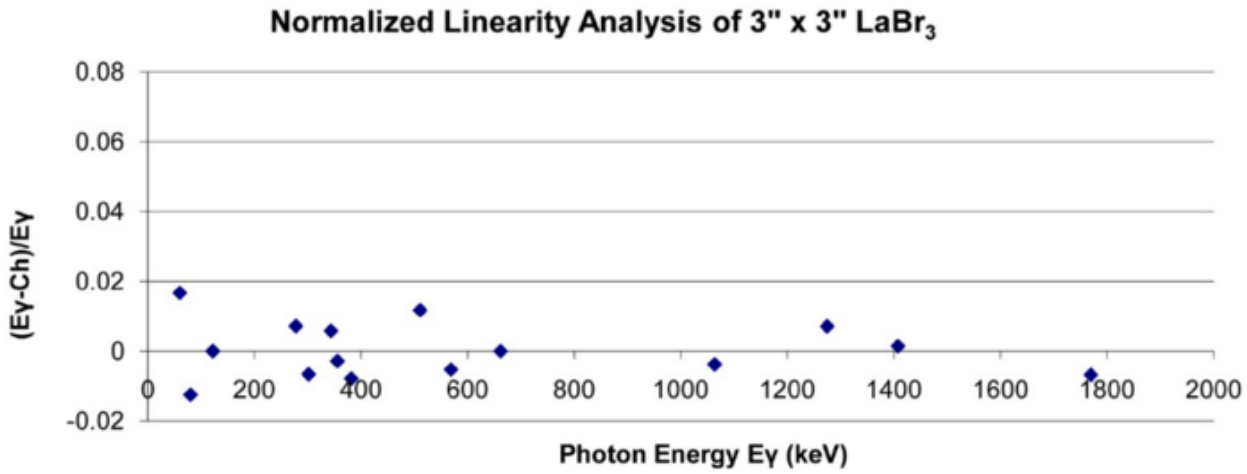

Figure 21. Normalized Linearity Analysis of the 3″ × 3″ $LaBr_3$:Ce detector. Here the difference of the photon energy and channel divided by the photon energy is plotted against the photon energy.

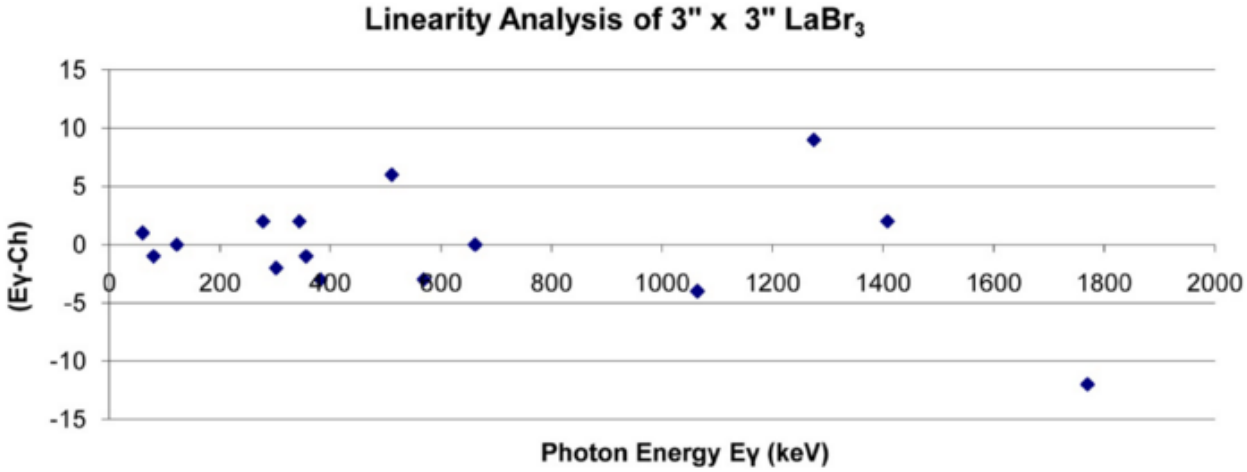

Figure 22. Linearity Analysis of the 3″ × 3″ $LaBr_3$:Ce detector. Here the difference of the photon energy and channel is plotted against the photon energy.

4. SUMMARY

This work started out as an investigation of room-temperature higher resolution detectors for use in extremely high sensitivity or signal low count rate nonproliferation missions. To that end, the results indicated that the $CeBr_3$ detector is as good as or better than the $LaBr_3$:Ce, $LaCl_3$:Ce, and NaI:Tl scintillator detectors when looking for very low count rate signatures of low energy SNM γ-rays. $CeBr_3$ appears to be an excellent alternative for $LaBr_3$:Ce, $LaCl_3$:Ce, and NaI:Tl scintillator detectors. It could also be a possible replacement for CZT Te in a variety of applications for γ-ray spectroscopy, in particular where moderate energy resolution and high detection efficiency is required. $CeBr_3$ has good linearity of response when compared to these other detectors. Also evident for the lanthanum halide detectors, for long counting times, are three intrinsic characteristic spectral lines (2 γ and 1 X-ray) and two 255 keV endpoint β spectra (one spectrum from 0 to 255 keV and the other from 789 to 1044 keV). These are associated with ^{138}La. However, being aware of these emission lines and β spectra, γ-ray spectroscopy using $LaBr_3$:Ce and $LaCl_3$:Ce should enable the experimenter to correct for many applications. However, for the most sensitive of measurements, best results with background in the energy regions associated with these ^{138}La-related self-activities can be obtained easily by replacing the lanthanum halide detector with $CeBr_3$. $CeBr_3$ scintillators can be used in a wide range of applications, such as coincidence counting, isotopic identification, and safeguards applications for monitoring of nuclear materials.

ACKNOWLEDGMENT

This manuscript has been authored by National Security Technologies, LLC, supported by the site-directed research and development program, under Contract No. DE-AC52-06NA25946 with the U.S. Department of Energy. The United States Government retains and the publisher by accepting the article for publication, acknowledges that the United States Government retains a non-exclusive, paid-up, irrevocable, worldwide license to publish or reproduce the published form of this manuscript, or allow others to do so, for United States Government purposes.

The authors acknowledge Mike Mayhugh from Saint-Gobain, for the development and growth of the detector material, and Jeanette Matthews, NSTec, for exceptional procurement support. UNLV contributed with construction of the Lead Shielding Pyramid, data acquisition, and analysis. Kanai Shah of Radiation Device, Inc. also presented advice as well as the original ½″ × ½″ $CeBr_3$ detector to Saint-Gobain, enabling this work.

REFERENCES

[1] Alexiev, D., Mo, L., Prokopovich, D. A., Smith, M. L., and Matuchova, M. "Comparison of $LaBr_3$:Ce and $LaCl_3$:Ce with NaI(Tl) and Cadmium Zinc Telluride (CZT) detectors," IEEE Trans. Nuc. Sci., 55(3), 1174 (2008).

[2] Guss, P. P., Reed, M., Yuan, D., Reed, A., and Mukhopadhyay, S., "CeBr3 as a High-Resolution Gamma-Ray Detector." NIM A 608, 297–304 (2009).

[3],Menge, P. R., Gautier, G., Iltis, A., Rozsa, C., and Solovyev, V., "Performance of large lanthanum bromide scintillators," Nucl. Instrum. Meth. Phys. Res A, 579, 6–10 (2007).

[4] Kernan, W. J., "Self-activity in lanthanum halides," IEEE Trans. Nucl. Sci., 53, 395–400 (2006).

[5] Balcerzyk, M., Moszynski, M., and Kapusta, M., "Comparison of LaCl : Ce and NaI(Tl) scintillators in γ-ray spectrometry," Nucl. Instrum. Meth. Phys. Res. A, 537, 50–56 (2005).

[6] Quarati, F., Bos, A.J.J., Brandenburg, S., Dathy, C., Dorenbos, P., Kraft, S., Ostendorf, R.W., Ouspenski, V., and Owens, A., "X-ray and gamma-ray response of a 2″ × 2″ LaBr:Ce scintillation detector," Nucl. Instrum. Meth. Phys. Res A, 574, 115–120 (2007).

[7] Mann, W. B., A. Rytz, and A. Spernol, "Radioactivity measurement; principles and practice," Appl. Radiat. Isotopes, 39, 717–737 (1988).

[8] International Atomic Energy Agency, Vienna, Austria, Tech. Rep. Ser. No.107, 1970.

[9] Arlt, R., Gryshchuk, V., and Sumah, P. "Gamma spectrometric characterization of various CdTe and CdZnTe detectors," Nucl. Instrum. Meth. Phys. Res. A, 428, 127–137 (1999).

[10] Shah, K.,Glodo, J., Higgins, W., van Loef, E.V.D., Moses, W.W., Derenzo, S.E., and Weber, M.J., "$CeBr_3$ scintillators for gamma-ray spectroscopy," *IEEE Trans. Nucl. Sci.* 52, 6, Part 2 3157–3159 (2005).

[11] Shah, K., Higgins, W., van Loef, E.V.D., "High Resolution Sensor for Nuclear Waste Characterization," *Final Report on DOE Contract DE-FG02-04ER84056*, Period of Performance: 7/13/04 – 4/12/05, SBIR data submitted to Denise Clarke, U.S. DOE/ACQ, Chicago Operations Office, 9800 South Cass Avenue, Argonne, IL. 60439. Radiation Monitoring Devices, Inc. (RMD), 44 Hunt St., Watertown, MA 02472. (2005). (http://www.er.doe.gov/sbir/awards_abstracts/sbirsttr/cycle22/phase1/161.htm).

[12] Shah, K., Radiation Monitoring Devices, Inc. (RMD), Watertown, MA 02472, private communication, January 23, 2007.

[13] Mukhopadhyay, S., "A High-resolution Gamma Ray Spectrometer at Room Temperature," *Nevada Test Site–Directed Research, Development, and Demonstration,* FY 2004, Bechtel Nevada, Las Vegas, Nevada, 145–151 (2005).

[14] Ra, S., S. Kim, H. J. Kim, H. Park, S. Lee, H. Kang, and S.-H. Doh, "Luminescence and scintillation properties of a $CeBr_3$ single crystal," *IEEE Trans. Nucl. Sci.,* 55(3), 1221–1224 (2008).

[15] van Eijk, C. W. E., Birowosuto, M. D., Bizarri, G., Dorenbos, P., de Haas, J. T. M., van der Kolk, E., Güdel, H., Krämer, K. "Recent Developments in the Inorganic Scintillator Field," presented at the International Workshop on Radiation Imaging Detectors (IWORID-7), Grenoble, France, July 4–7, 2005.